International Journal of Nanoelectronics and Materials

In Press, Accepted Manuscript – Note to user

Structural, Optical and I-V Characteristics of ITO/p-Si Hetero-junction deposited by chemical Spray Pyrolysis

Salam Amir Yousif[1*], Duha Ismail Khalil[1]

Physics Department, College of Education, Mustansiriyah University, Baghdad - Iraq

ABSTRACT

__I__ndium __T__in __O__xide (ITO) thin films at different tin doping of 0, 5, 10, 15, 20 wt% were successfully prepared by chemical spray pyrolysis (CSP) method. The peaks of XRD indicate that all samples have polycrystalline cubic structure and the plane (222) is the preferential orientation. AFM examinations show that the root mean square roughness of ITO thin films decreased with increasing tin doping and the grain size transformed from microstructure to nanostructure when tin doped with indium oxide. The maximum transmittance value measured is approximately 80% for infrared region, and the band gap is equal to 3.5, 3.7, 3.67, 3.65, 3.58eV corresponding to the concentration 0, 5, 10, 15, 20%. I-V characteristics of ITO/p-Si hetero-junction for dark and illuminated conditions have been investigated.

Keywords: ITO thin film, Structural properties, Optical properties, I-V Characteristics, Spray pyrolysis

1. INTRODUCTION

ITO is n-type transparent conducting oxides material. Because it has large optical transparency, low resistivity and energy band gap of larger than 3.5 eV, it can be extensively applied in different technological applications like antireflection coatings [1] solar cells [2, 3], liquid crystal displays [4], photocurrent generators [5], light emitting diodes [6, 7] and gas sensors [8]. The ITO films are usually fabricated utilizing different methods like sputtering [9-11], sol-gel technique [12-14], vacuum thermal evaporation [15], pulsed laser deposition [16,17], chemical vapor deposition [18,19] and chemical spray pyrolysis [20-25].

Tirumoorthi and Prakash [26] were prepared ITO thin films on glass substrate by CSP method at different tin content, the physical properties of these films have been studied. They are showed that ITO films are polycrystalline cubic structure and they are detected a transfer of the preferential construction from [400] direction for un-doped films to [222] direction for doped films. The roughness and root mean square are decreased with increased tin content and the optical transmittance was improved from 77% to 87%. The carrier concentration increased, the resistivity reduced and there is an improvement in the mobility when tin doping in indium oxide. Yoo and Lee [27] were studied the effect of annealing temperature on the electrical properties of ITO/n-type and p-type Si wafers Schottky junction using Rf magnetron sputtering technique. They were found that a layer with positive charges is created between ITO film and silicon wafer and it can be removed (positive fixed charges) by heat treatment. The Schottky barrier of ITO/n-Si increased after annealing process and the barrier of ITO/p-Si decreased after annealing process.

*Email of corresponding author: salammomica@yahoo.com

In this paper, study the capability of prepare indium tin oxide thin films with high uniformity and good quality using CSP method, and if the ITO is suitable for optoelectronic application to produce ITO/p-Si photo-detector.

2. EXPERIMENTAL PART

Indium tin oxide films at different tin doping were fabricated on glass slides at a substrate temperature equals to (450 ± 10)°C using chemical spray pyrolysis (SP) technique as shown in figure (1). To prepare the sprayed solution, Indium Chloride $InCl_3$ (98% purity, Thomas Baker, India), Stannic Chloride $SnCl_4.5H_2O$ (99% purity, Chemical Point, Germany) and distilled water were mixed thoroughly to get the sprayed solution with a concentration of 0.05 $(mole/liter)$ and, hydrochloric (HCl) acid was added to the mixture to get a homogeneous and clear solution. Before deposition, glass substrates were cleaning ultrasonically in distilled water for 15 minutes and then the previous step was repeated with pure alcohol and pure acetone solution. The slides were desiccate via an air blower. The slides utilized for ITO/p-Si hetero-junction is mono-crystalline p-Si with the resistivity equal to (1.5-4) $\Omega.cm$ and $\langle 111 \rangle$ direction with thickness equal to $(508 \mp 15)\mu m$. Before the deposition process, Si slides were treated by the same above steps. One side of the Si surface was previously mechanically polished like mirror. Native oxides were removed by 40:60 HF:H_2O solution. The size of photo detector is $(10\ mm \times 10\ mm)$.

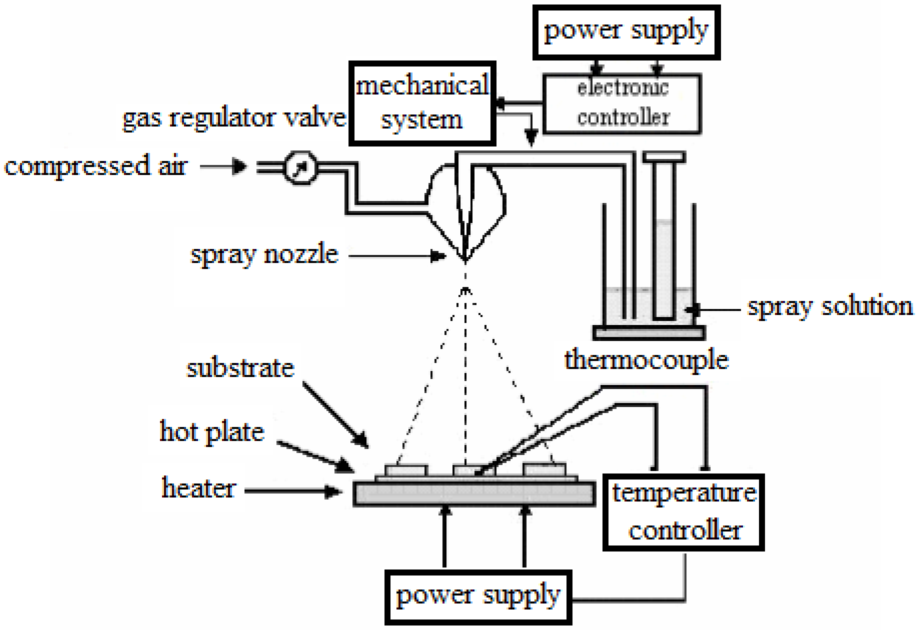

Figure 1. Graphical representation of CSP unit.

X-ray diffraction (XRD) instrument kind (Shimadzu 6000) was utilized to investigate the structural properties of the samples. Morphological parameters of the samples were examined employing (SPM AA3000 Angstrom Advanced Inc.). Ultraviolet - Visible spectrophotometer (Shimadzu UV-1650 PC) have been used to measuring the optical parameters of ITO films from the transmittance and absorbance spectra at wavelength interval from 300 to 1000 nm. The current-voltage characteristics of ITO/p-Si photo detector have been tested successfully using the following setup.

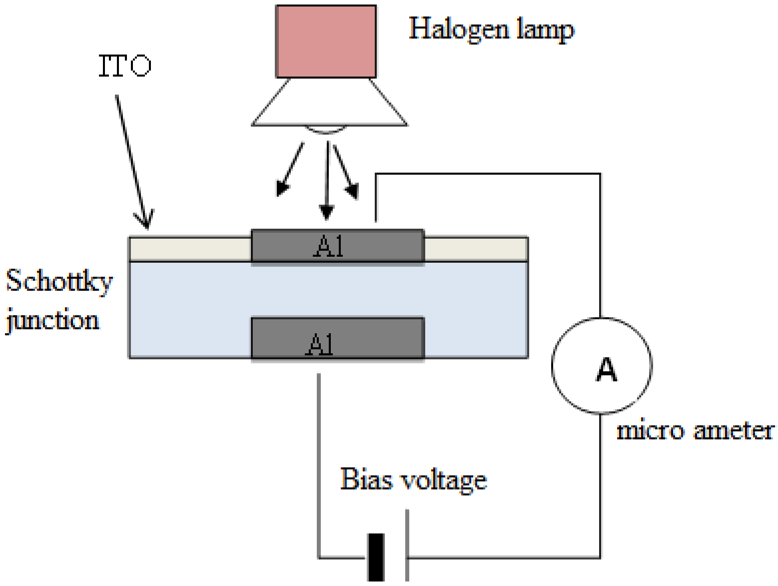

Figure 2. Schematic diagram of (I-V) characteristics setup.

3. RESULTS AND DISCUSSION

3.1 Structural properties

Figure (3) illustrates the XRD pattern of indium tin oxide for various tin doping of 0, 5, 10, 15, 20 wt% and has been indexed with JCPDS (card 06-0416 $In_2O_3, cubic$). The presence of diffraction peaks indicates that the samples are polycrystalline cubic structure. The XRD measurements revealed that the In_2O_3 samples show a peak (400) as a highest intensity with a texture coefficient equal to 2.8418 as a preferred growth orientation, while the doped films have the peak (222) as the highest intensity, in other word, there are a converting in the construction direction from [400] to [222] while Sn added to the In_2O_3. The transformation of preferential direction growth can be explained by occupation of tin atoms in the indium vacancy sites that unoccupied already. This result is corresponds with another research [26]. The intensity of (222) peak rise with rising tin content in ITO samples and the intensity of (400) peak decreases with rising tin content in the samples. The rises of preferred direction growth are connected with the rises of the growth of crystallite film. The values of full width at half maximum (FWHM)(β), lattice constant (a), crystallite size (D), dislocation density (δ), strain ($\varepsilon_\circ$) and texture coefficient (TC) of ITO thin films have been calculated employing the following theoretical equations and are listed in Table (1).

The lattice parameter (a) of cubic structure is given by:

$$a = \frac{d}{\sqrt{h^2+k^2+l^2}} \tag{1}$$

Where (d): is the spacing between planes and (hkl): miller indices of that plane.

By using Debye-Scherrer equation [28], we can calculate the size of the crystallite (D) as:

$$crystallite\ size\ (D) = \frac{0.9 \times wave\ length\ (\lambda)}{FWHM\ (\beta) \times cos\theta} \tag{2}$$

Where the wavelength of the incident x-ray beam ($\lambda = 1.5406$ Å), (β) is given (in radian) and finally (θ) represent the Bragg's angle (in degree).

Relations (3) and (4) have been used to calculate the dislocation density (δ) and the strain ($\varepsilon_\circ$) [28]:

$$\delta = \frac{1}{D^2} \tag{3}$$

$$\varepsilon_\circ = \frac{\beta\, COS\theta}{4} \tag{4}$$

Relation (5) shows the texture coefficient (TC) of the samples which explain the direction of preferential growth [29]:

$$T_c(hkl) = \frac{I(hkl)/I_0(hkl)}{N_r^{-1}\sum I(hkl)/I_0(hkl)} \tag{5}$$

Where $I(hkl)$ is the measured intensity, $I_0(hkl)$ is the standard intensity according to the JCPDS (card 06- 0416 $In_2O_3, cubic$) and N_r is the number of diffraction peaks presented.

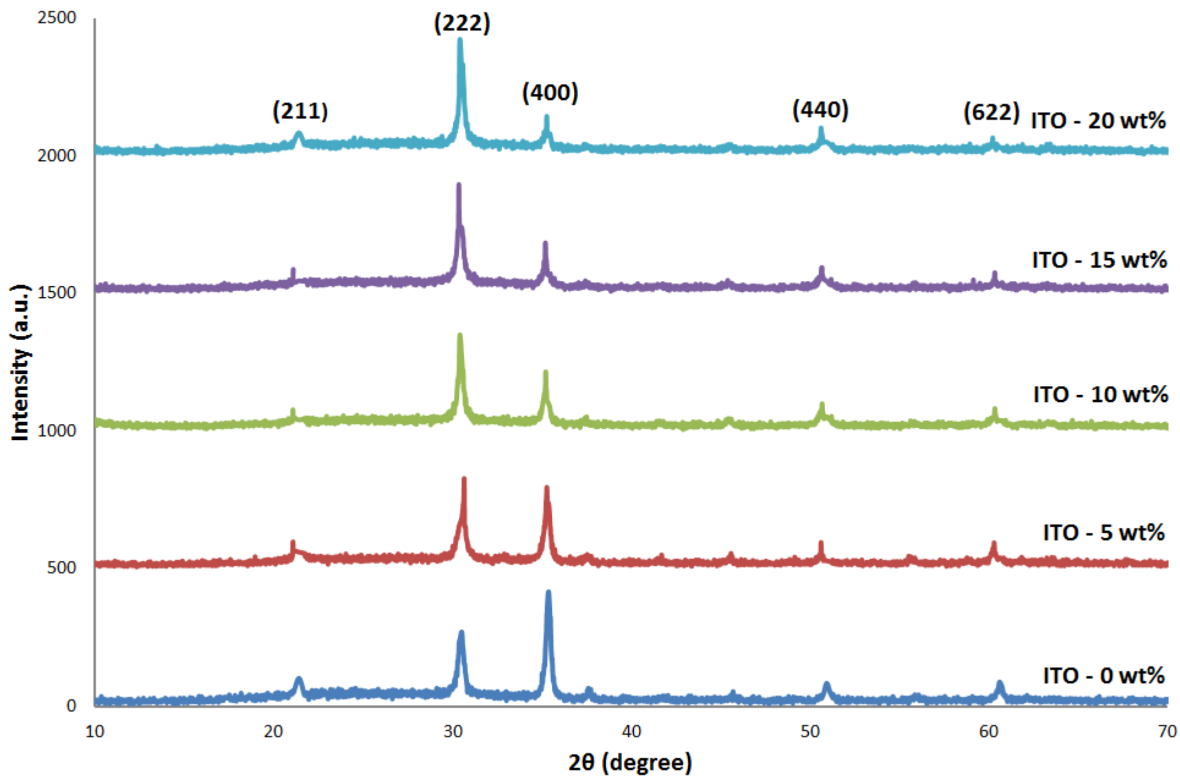

Figure 3. XRD pattern of ITO thin films at different tin doping**.**

Also, figure (3) shows a slightly shift of (222) and (444) peaks across smaller angle (2θ) which is because the alteration of tin ion in indium sites which cause the variation of strain in the lattice which corresponds with the report [30].

Table 1 Some structural parameters of $In_2O_3:Sn$ films

Tin-dopign wt%	hkl	FWHM (deg)	D (nm)	δ line/m² (10^{15})	ε∘ (10^{-3})	Lattice parameter (Å)	texture coefficient TC
0	*211*	*0.32000*	*25.2*	*1.57*	*1.37*	*10.16*	*0.6698*
	222	*0.33380*	*24.6*	*1.65*	*1.40*	*10.15*	*0.5285*
	400	*0.30140*	*27.6*	*1.31*	*1.25*	*10.14*	*2.8418*
	440	*0.27600*	*31.8*	*0.98*	*1.08*	*10.13*	*0.4140*
	622	*0.29470*	*31.2*	*1.02*	*1.11*	*10.12*	*0.5456*
5	*211*	*0.35500*	*22.7*	*1.94*	*1.52*	*10.15*	*0.7662*
	222	*0.40710*	*20.2*	*2.45*	*1.71*	*10.14*	*0.8252*
	400	*0.35480*	*23.5*	*1.81*	*1.47*	*10.13*	*2.1730*
	440	*0.41330*	*21.2*	*2.22*	*1.62*	*10.13*	*0.5422*
	622	*0.40170*	*22.9*	*1.90*	*1.51*	*10.12*	*0.6931*
10	*211*	*0.36000*	*22.4*	*1.99*	*1.54*	*10.16*	*0.8218*
	222	*0.40180*	*20.4*	*2.40*	*1.69*	*10.15*	*1.0460*
	400	*0.36670*	*22.7*	*1.94*	*1.52*	*10.14*	*1.6736*
	440	*0.35600*	*24.7*	*1.63*	*1.40*	*10.13*	*0.7471*
	622	*0.39500*	*23.2*	*1.85*	*1.48*	*10.13*	*0.7112*
15	*211*	*0.35340*	*22.8*	*1.92*	*1.51*	*10.18*	*0.7889*
	222	*0.40600*	*20.2*	*2.45*	*1.70*	*10.16*	*1.1045*
	400	*0.34760*	*23.9*	*1.75*	*1.44*	*10.15*	*1.7304*
	440	*0.41330*	*21.2*	*2.22*	*1.62*	*10.14*	*0.7574*
	622	*0.40600*	*22.6*	*1.95*	*1.53*	*10.14*	*0.6185*
20	*211*	*0.32660*	*24.7*	*1.63*	*1.40*	*10.15*	*0.8568*
	222	*0.36850*	*22.3*	*2.01*	*1.55*	*10.14*	*1.3328*
	400	*0.35130*	*23.7*	*1.78*	*1.46*	*10.14*	*1.3328*
	440	*0.46500*	*18.9*	*2.79*	*1.83*	*10.13*	*0.8377*
	622	*0.53500*	*17.1*	*3.41*	*2.01*	*10.13*	*0.6397*

3.2 Topography properties

Three dimensional AFM pictures of $In_2O_3:Sn$ samples at various tin doping are illustrated in figure (4). Table (2) shows that the AFM parameters are varied with rising tin doping. It is observed that the roughness of ITO samples decreases from 4.68 to 2 nm with rising tin content in the samples, because the lowering in the vacancy defects and the rearrangement of atoms in the samples. The morphological measurements show that the samples have highly uniformity surface and such surface can be used in solar cells or photo-detector.

The grain size (D) values of ITO samples are changing as 107, 95, 96, 100, 77nm for tin content 0, 5, 10, 15, 20 wt% respectively. The size of the grains transformed from microstructure to nanostructure when tin doped with indium oxide. AFM study reveals that the grain size and the surface roughness of ITO samples are strongly dependent on the concentration of the tin content in the samples.

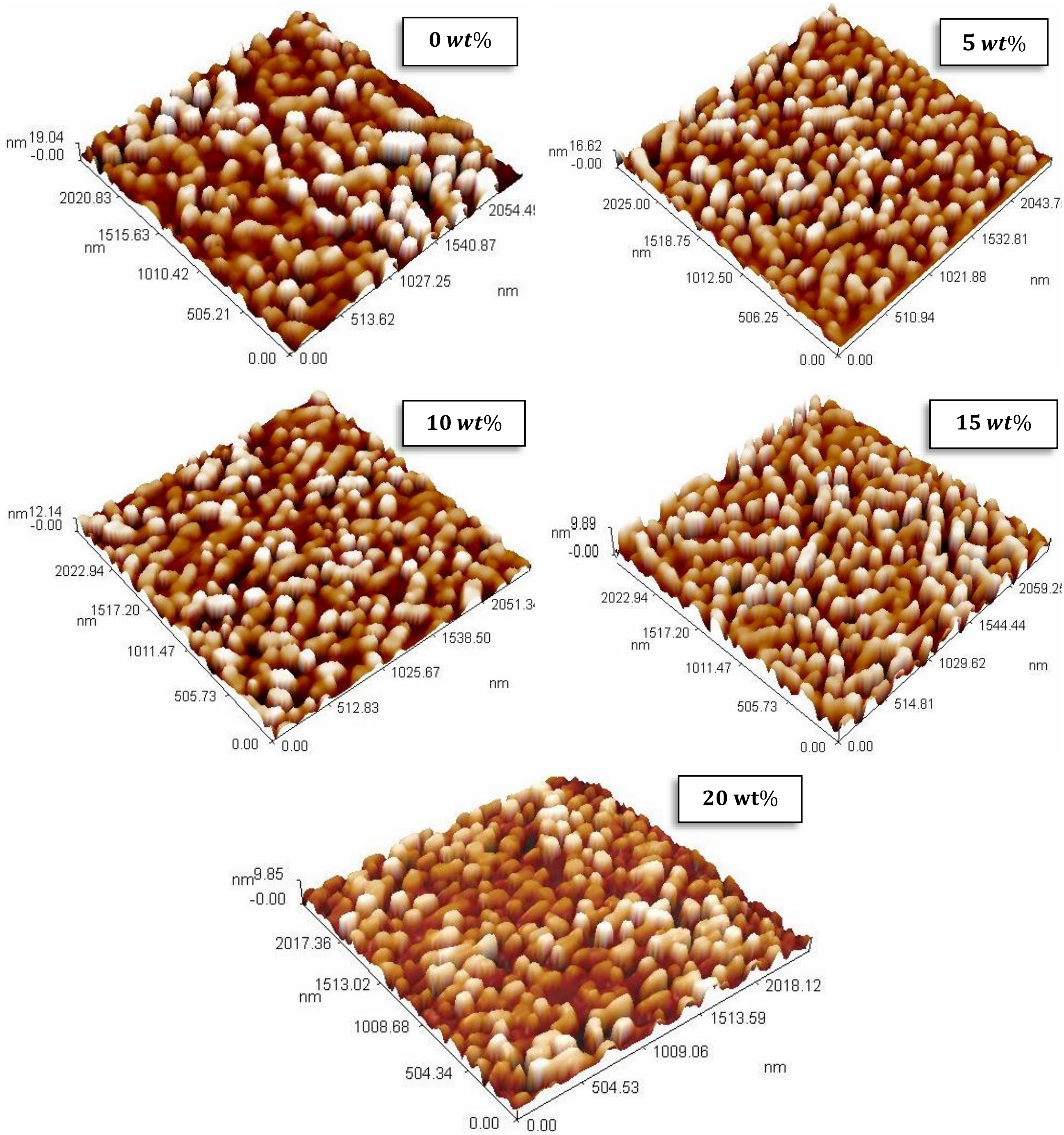

Figure 4. AFM images of ITO thin films at different tin doping.

Table 2 Morphological parameters of ITO films

Tin content	Root Mean Square roughness (nm)	Gain size (nm)
0 wt%	4.68	107
5 wt%	3.56	95
10 wt%	2.75	96
15 wt%	2.3	100
20 wt%	2	77

3.3 Optical properties

The transmittance and absorbance spectrum of ITO samples were calculated at 27 °C in the range from (300 - 1000) nm. Figure (5) shows that the transmittance of ITO samples rise with rising tin concentration up to 5%. Thereafter, it goes on decreases gradually with rising tin concentration at 10, 15, 20%. The transmittance of ITO samples decreases after addition a large amount of impurity caused by rising scattering of photons resulted from crystal defects (impurities), which is in compatible with report [31]. Figure (6) illustrate the absorbance curves of ITO films as a function of calculated wavelength.

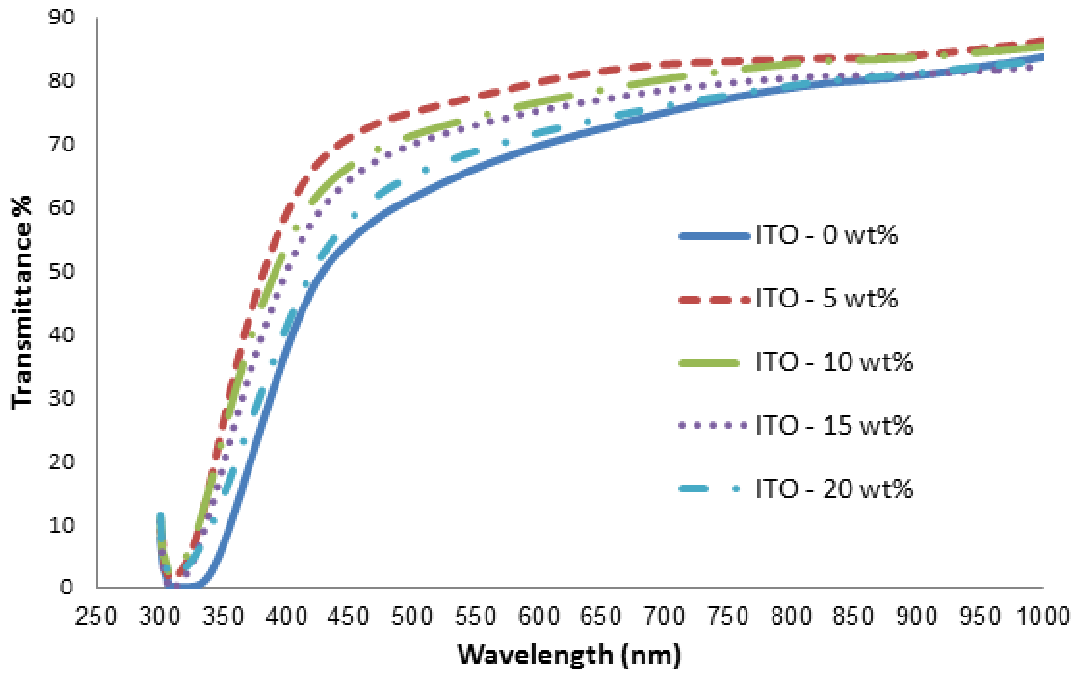

Figure 5. Transmittance spectra of ITO thin films.

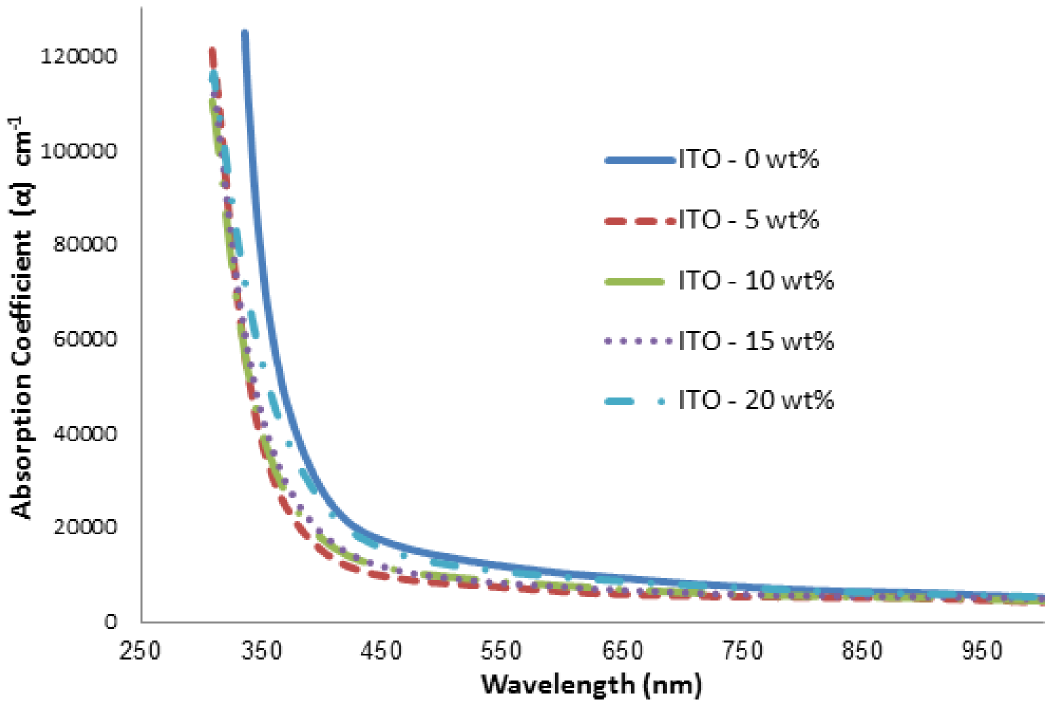

Figure 6. Absorption coefficient of ITO thin films.

Equation (6) shows the relation of absorption coefficient and photon energy (hγ) for direct transition [28]:

$$\alpha h\gamma = A(h\gamma - E_g)^X \tag{6}$$

Where (hγ) is the photon energy, (E_g) is the energy band gap and (A) is constant.

The optical band gap of ITO thin films is found to be 3.5, 3.7, 3.675, 3.65, 3.58eV corresponding to the tin content. The optical band gap of ITO samples rise with rising tin content up to 5%, due to the rises of carrier density with rising tin content, then it reduction for further rising in tin content from 5 to 20%, we can be explain this behavior by formation of donor levels near the conduction band in the energy gap caused by the impurities that lead to absorb low energy photons [32].

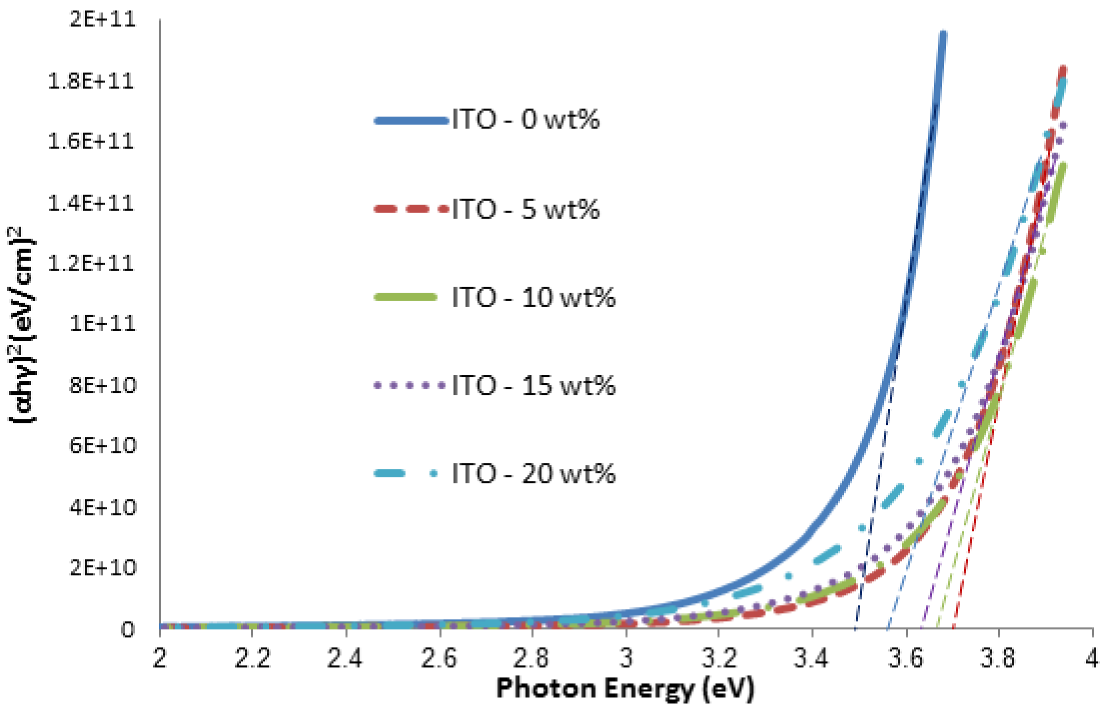

Figure 7. Variation of $(\alpha h\gamma)^2$ vs. photon energy $(h\gamma)$ for ITO thin films at different tin doping.

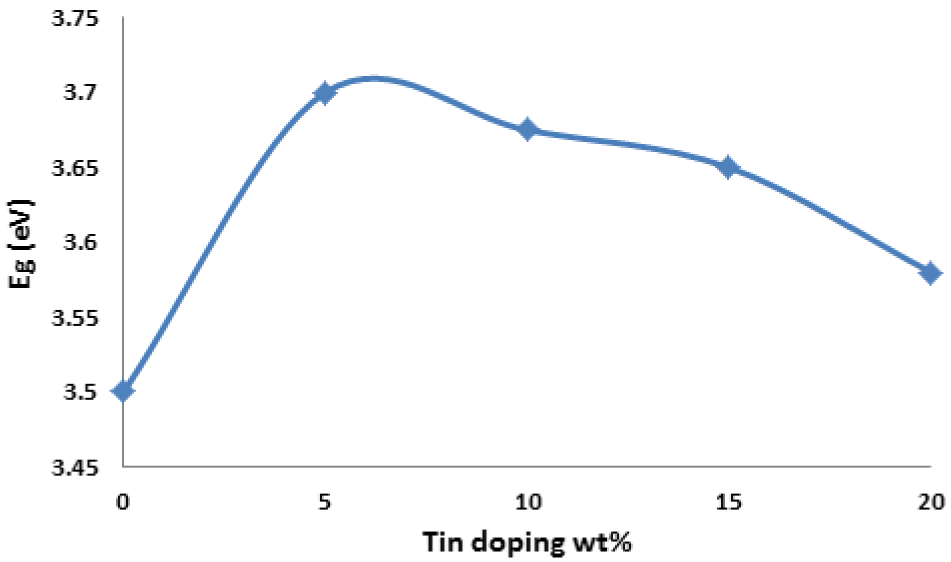

Figure 8. Energy band gap (E_g) of ITO thin films as a function of tin doping.

3.4 I-V Characteristics

I-V characteristics of ITO/p-Si hetero-junction have been investigated under dark conditions as shown in figure (9). In practice, the diode does not exactly obey the theoretical diode relation. The ideality factor (B) of can be calculated using the following equation and listed in table (3):

$$B = \frac{q}{K_B T} \frac{V}{\ln\frac{I}{I_s}} \tag{7}$$

Where: V is the forward bias voltage, K_B is Boltzmann constant and I_s is the saturation current.

It is known, that the reverse bias current increased after illuminating the ITO/p-Si junction because the electron – hole pairs are created in the depletion region if the energy of incident photon is greater than the direct energy band gap of the ITO/p-Si hetero-junction. Figure (10) shows current – voltage relation of ITO/p-Si hetero-junction for murky and shining conditions at reverse bias.

Where the current under murky condition can be noted by (I_d), the current under shining condition can be noted by (I_t) so the photocurrent giving by:

$$(I_{ph} = I_t - I_d) \tag{8}$$

it can be seen clearly that the photocurrent (I_{ph}) rise with rising tin content up to 5%, then it reduction for further rising of tin content in the samples, because, the optical band gap of the films rise with rising tin content up to 5% and then begin to decreases with the rising tin content in the films.

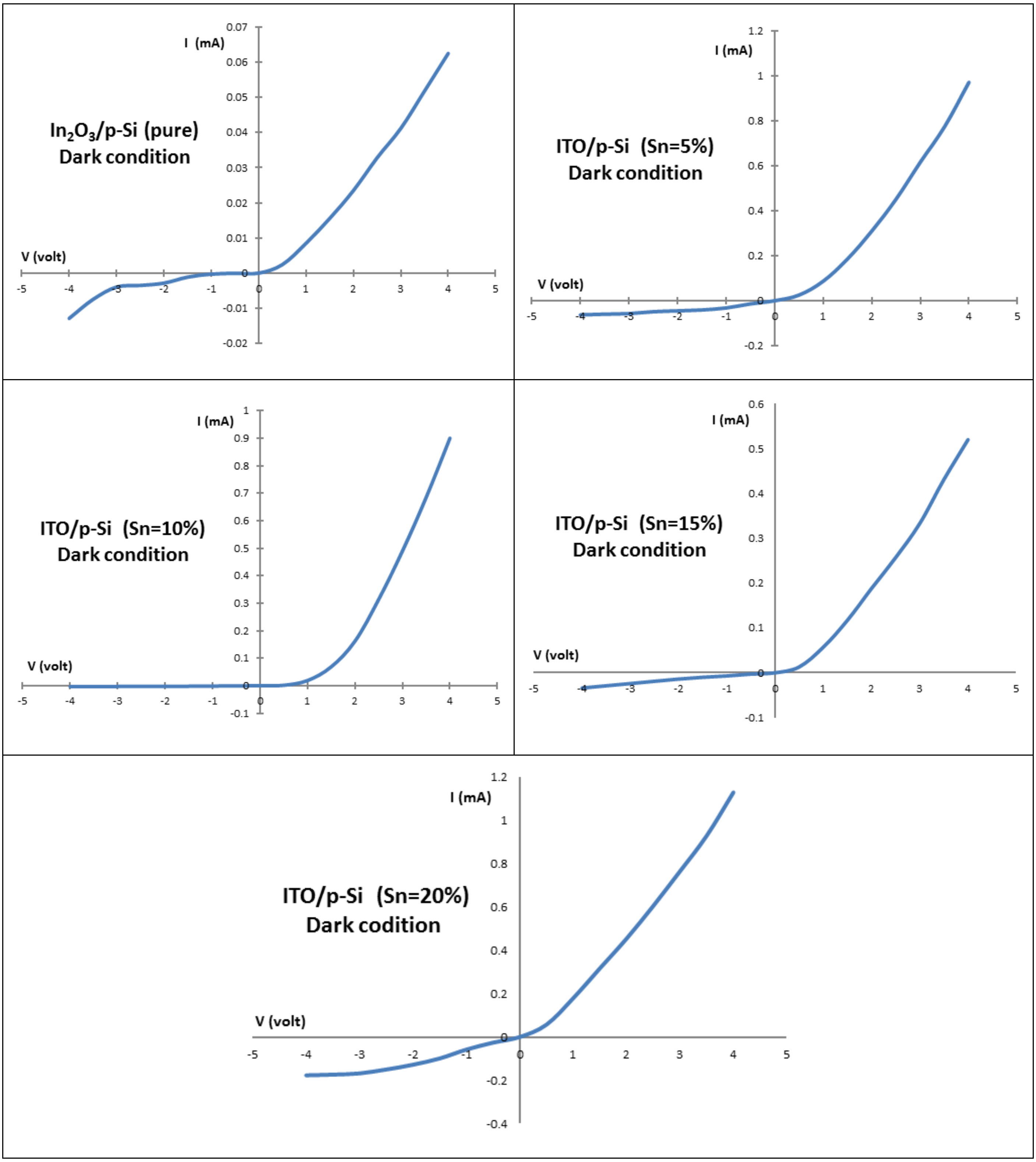

Figure 9. I-V curve of ITO/p-Si Heterojunction under dark condition

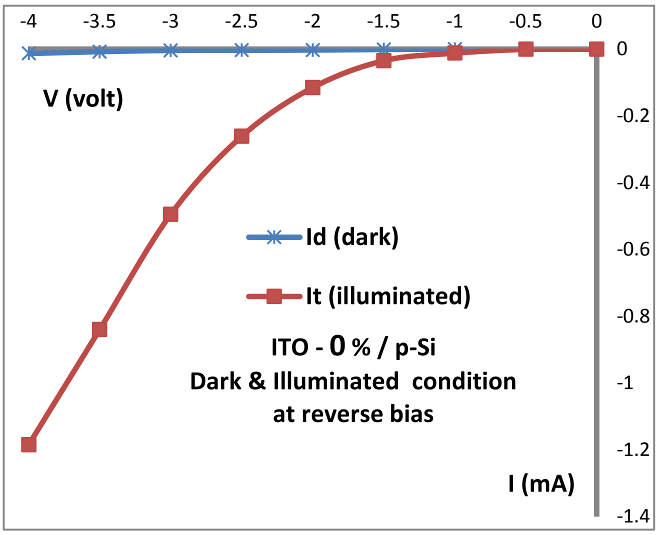
-4
-3.5
-3
-2.5
-2
-1.5
-1
-0.5
0
V (volt)
0
-0.2
-0.4
-0.6
-0.8
-1
-1.2
-1.4
Id (dark)
It (illuminated)
ITO - 0 % / p-Si
Dark & Illuminated condition
at reverse bias
I (mA)

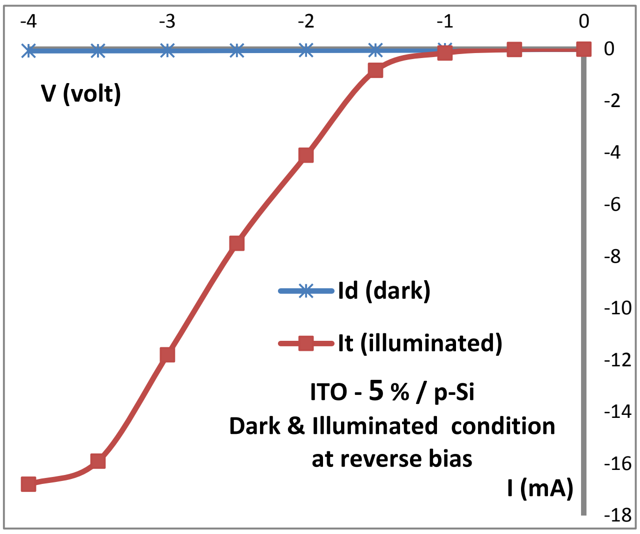
-4
-3
-2
-1
0
V (volt)
0
-2
-4
-6
-8
-10
-12
-14
-16
-18
Id (dark)
It (illuminated)
ITO - 5 % / p-Si
Dark & Illuminated condition
at reverse bias
I (mA)

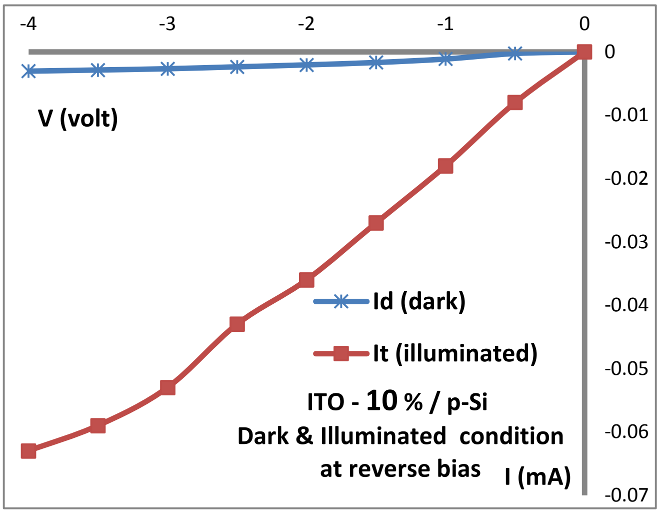
-4
-3
-2
-1
0
V (volt)
0
-0.01
-0.02
-0.03
-0.04
-0.05
-0.06
-0.07
Id (dark)
It (illuminated)
ITO - 10 % / p-Si
Dark & Illuminated condition
at reverse bias
I (mA)

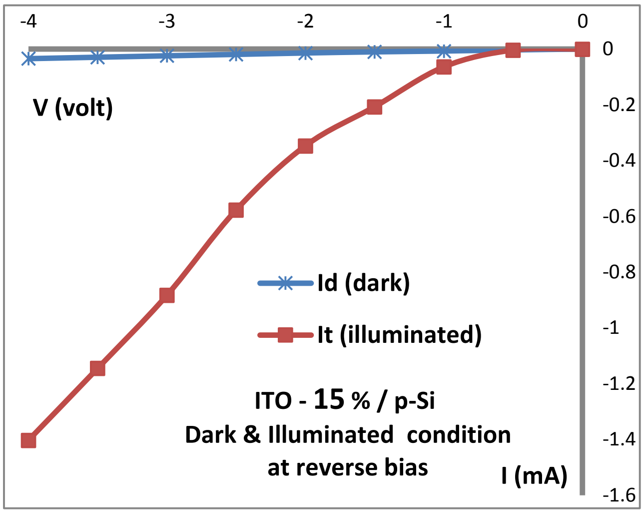
-4
-3
-2
-1
0
V (volt)
0
-0.2
-0.4
-0.6
-0.8
-1
-1.2
-1.4
-1.6
Id (dark)
It (illuminated)
ITO - 15 % / p-Si
Dark & Illuminated condition
at reverse bias
I (mA)

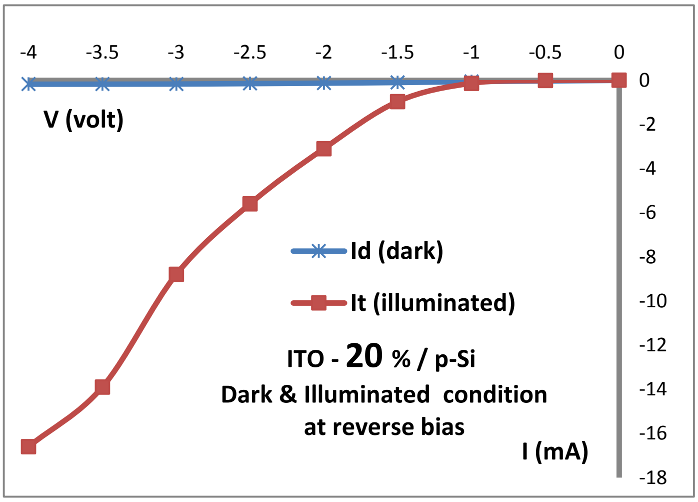
-4
-3.5
-3
-2.5
-2
-1.5
-1
-0.5
0
V (volt)
0
-2
-4
-6
-8
-10
-12
-14
-16
-18
Id (dark)
It (illuminated)
ITO - 20 % / p-Si
Dark & Illuminated condition
at reverse bias
I (mA)

Figure 10. I-V curve of ITO/p-Si hetero-junction under dark and illuminated condition at reverse bias voltage.

The spectral response of ITO/p-Si hetero-junction for white light has been calculated using the following equation and listed in table (3):

$$R_\lambda = \frac{I_{ph}}{P_{in}} \ (A/W) \qquad (9)$$

Where: I_{ph} is the photocurrent and P_{in} is the input power.

Table 3 Ideality factor and Spectral response of ITO/p-Si hetero-junction

Sn – content wt%	Ideality Factor (B)	Spectral Response (A/W) at 550 nm
0	6.63	1.1215
5	4	4.055
10	1.7	3.396
15	2.9	3.33
20	6.1	2.972

From current – voltage characteristics of ITO/p-Si hetero-junction we can be noted that $In_2O_3:Sn$ films deposited by chemical spray pyrolysis method are suitable for optoelectronic application such as solar cells and photodetectors.

4. CONCLUSION

Indium tin oxide (ITO) thin films were successfully prepared on glass and p-type silicon substrates by CSP method. The effect of tin concentration on the structural, morphological, optical and I-V characteristic of ITO/p-Si hetero-junction have been investigated. After these studies, we conclude that there is a converting in the construction direction from [400] to [222] direction while Sn added to the In_2O_3 confirms the substitution of tin in indium-Oxide lattice. The rms roughness values are decreased with rising tin doping concentration and the grain size transformed from microstructure to nanostructure when tin doped with indium oxide. The optical band gap rises from 3.5eV at (0 wt%) to 3.7eV at (5 wt%) and then decreased to 3.58eV at (20 wt%), the rises of optical band gap with rising carrier concentration is explained by applied Moss-Burstein theory. The reducing of energy band gap for larger tin content concentration because the effects of interaction through free carriers and ionized impurities or through free carriers. From our results we deduce that indium tin oxide films can be manufacturing by chemical spray pyrolysis method with uniform, homogeneous and good quality films. ITO thin films are appropriate for optoelectronic application especially for ITO/p-Si photo-detector.

ACKNOWLEDGEMENTS

We would like to thank Mustansiriyah University – College of Education for their help and support on this work.

REFERENCES

[1] S. A. Yousif, H. G. Rashid, K. A. Mishjil and N. F. Habubi, "Design and Preparation of Low Absorbing Antireflection Coatings Using Chemical Spray Pyrolysis" International Journal of Nanoelectronics and Materials *Volume* **11**, No. 4, (2018) 449-460.

[2] K. Yamamoto, M. Yoshimi, Y. Tawada, Y. Okamoto, A. Nakajima and S. Igari, "Thin-film poly-Si solar cells on glass substrate fabricated at low temperature", Appl. Phys. A **69** (1999) 179-185.

[3] D. Gebeyehu, C. J. Brabec, N. S. Sariciftci, D. Vangeneugden, R. Kiebooms, D. Vanderzande, F. Kienberger and H. Schindler,"Hybrid solar cells based on dye-sensitized nanoporous TiO_2 electrodes and conjugated polymers as hole transport materials" Synth. Met. **125** (2001) 279-287.

[4] J. C. Manifacier, "Thin metallic oxides as transparent conductors", Thin Solid Films **90** (1982) 297-308.

[5] W. J. Lee, R. S. Mane, S. H. Lee and S. H. Han, "Enhanced photocurrent generations in $RuL_2(NCS)_2$/di-(3-aminopropyl)-viologen self-assembled on In_2O_3 nanorods", Electrochem. Commun. **9** (2007) 1502-1507.

[6] S. T. Lee, Z. Q. Gao and L. S. Hung, "Metal diffusion from electrodes in organic light-emitting diodes", Appl. Phys. Lett. **75** (1999) 1404.

[7] H. Kim, C. M. Gilmore, A. Pique, J. S. Horwitz, H. Mattoussi, H. Murata, Z. H. Kafafi and D. B. Chrisey, "Electrical, optical, and structural properties of indium–tin–oxide thin films for organic light-emitting devices", J. Appl. Phys. **86** (1999) 6451.

[8] N. G. Patel, P. D. Patel, V. S. Vaishnav,"Indium tin oxide (ITO) thin film gas sensor for detection of methanol at room temperature", Sensors and Actuators B: Chemical **96** (2003) 180-189.

[9] J. H. Park, C. Buurma, S. Sivananthan, R. Kodama, W. Gao and T. A. Gessert,"The effect of post-annealing on Indium Tin Oxide thin films by magnetron sputtering method" Appl. Surf. Sci. **307** (2014) 288-392.

[10] L. Dong, G. Zhu, H. Xu, X. Jiang, X. Zhang, Y. Zhao, D. Yan, L. Yuan and A. Yu," Fabrication of Nanopillar Crystalline ITO Thin Films with High Transmittance and IR Reflectance by RF Magnetron Sputtering" Materials **12** (2019) 958.

[11] K. C. Heo, Y. K. Sohn and J. S. Gwag, "Effects of an additional magnetic field in ITO thin film deposition by magnetron sputtering" Ceram. Int. **41** (2015) 617-621.

[12] Y. Wang, J. Liu, X. Wu and B. Yang, "Adhesion enhancement of indium tin oxide (ITO) coated quartz optical fibers" Appl. Surf. Sci. **308** (2014) 341-346.

[13] M. T. Kesim and C. Durucan, "Indium tin oxide thin films elaborated by sol-gel routes: The effect of oxalic acid addition on optoelectronic properties" Thin Solid Films **545** (2013) 56-63.

[14] L. Korosi, S. Korosi and I. Dekany, "Preparation of transparent conductive indium tin oxide thin films from nanocrystalline indium tin hydroxide by dip-coating method" Thin Solid Films **519** (2011) 3113-3118.

[15] K. -Y. Pan, L. -D. Lin, L. -W. Chang and H. C. Shih, "Studies on the optoelectronic properties of the thermally evaporated tin-doped indium oxide nanostructures" Appl. Surf. Sci. **273** (2013) 12-18.

[16] J. B. Choi, J. H. Kim, K. A. Jeon and S. Y. Lee, " Properties of ITO films on glass fabricated by pulsed laser deposition" Mater. Sci. Eng. **102** (2003) 376-379.

[17] J. M. Dekkers, G. Rijnders and D.H. A. Blank, "Role of Sn doping in In_2O_3 thin films on polymer substrates by pulsed-laser deposition at room temperature" Appl. Phys. Lett. **88** (2006) 151908.

[18] Y. C. park, Y. S. Kim, H. K. Seo, S. G. Ansari and H. S. Shin, "ITO thin films deposited at different oxygen flow rates on Si(100) using the PEMOCVD method" Surf. Coat. Technol. **161** (2002) 62-69.

[19] Y. S. Kim, Y. C. Park, S. G. Ansari, B. S. Lee and H. S. Shin, "Effect of substrate temperature on the bonded states of indium tin oxide thin films deposited by plasma enhanced chemical vapor deposition" Thin Solid Films **426** (2003) 124-131.

[20] G.G. Untila, T.N. Kost, A.B. Chebotareva, "Fluorine- and tin-doped indium oxide films grown by ultrasonic spray pyrolysis: Characterization and application in bifacial silicon concentrator solar cells" Solar Energy **159** (2018) 173–185.

[21] R. Rana, J. Chakraborty, S. K. Tripathi, M. Nasim**, "**Study of conducting ITO thin film deposition on flexible polyimide substrate using spray pyrolysis**"** J Nanostruct Chem **6** (2016) 65–74.

[22] K. Navya, S.P. Bharath, K. V. Bangera, G.K. Shivakumar, "Effect of indium content on the characteristics of indium tin oxide thin films" Mater. Res. Express **5** (2018) 096410.

[23] L. Zhang, J. Lan, J. Yang, S. Guo, J. Peng, L. Zhang, S. Tian, S. Ju, W. Xie, "Study on the physical properties of indium tin oxide thin films deposited by microwave-assisted spray pyrolysis "Journal of Alloys and Compounds 728 (2017) 1338-1345.

[24] A. R. Babar, S. S. Shinde, A. V. Moholkar, C. H. Bhosale, J. H. Kim and K. Y. Rajpure, "Sensing properties of sprayed antimony doped tin oxide thin films: Solution molarity" J. Alloys Compd. **509** (2011) 3108-3115.

[25] K. Ravichandran and K. Thirumurugan, "Type Inversion and Certain Physical Properties of Spray Pyrolysed SnO_2:Al Films for Novel Transparent Electronics Applications"J. Mater. Sci. Technol. **30** (2014) 97-102.

[26] M. Thirumoorthi and J. Thomas Joseph Prakash,"Structural, optical and electrical properties of indium tin oxide ultra-thin film prepared by jet nebulizer spray pyrolysis technique", Journal of Asian Ceramic Societies **4** (2016) 124-132.

[27] Keon Yoo, and Jong-Ho Lee, "Effect of Low Temperature Annealing on ITO-on-Si Schottky Junction" IEEE ELECTRON DEVICE LETTERS **38** (2017) 426-429.

[28] M. Thirumoorthi and J. Thomas Joseph Prakash," Structural, morphological characteristics and optical properties of Y doped ZnO thin films by sol-gel spin coating method" Superlattices and Microstructures **85** (2015) 237-247.

[29] S. S. Shinde, P. S. Shinde, S. M. Pawar, A. V. Moholkar, C. H. Bhosale and K. Y. Rajpure, "Studies on pure and fluorine doped vanadium pentoxide thin films deposited by spray pyrolysis technique" Solid State Sci. **10** (2008) 1209-1214.

[30] G. B. Gonzalez, J. B. Cohen, J. H. Hwang, T. O. Mason, J. P. Hodges and J. D. Jorgensen, "Neutron diffraction study on the defect structure of indium-tin-oxide", J. Appl. Phys. **89** (2001) 2550-2555.

[31] A. H. Al-hamdani, ''Structural and Optoelectronic Properties of Nanostructured ITO Thin Films Deposited by Chemical Spray Pyrolysis Technique'', Journal of Materials Science and Engineering **12** (2014) 346-352.

[32] S. D. M AL-Algawi, S. H Al-Jawad and N. M. Saadoon,''Physical Properties of Indium Tin Oxide (ITO) Nanopartical Thin Films Used as Gas Sensor'', Eng. &Tech. Journal **33** (2015) 141-15.